sustainability

MDPI

Article

Study on Migratory Behavior of Aggregate in Asphalt Mixture Based on the Intelligent Acquisition System of Aggregate Attitude Data

Chen Zhang [1,2,*] and Zhengwei Zhang [1]

1 School of Energy and Architecture, Xi'an Aeronautical University, Xi'an 710077, China
2 Key Laboratory for Special Area Highway Engineering of Ministry of Education, Chang'an University, Xi'an 710064, China
* Correspondence: zlw19861108@aliyun.com

Abstract: In order to provide a new method to study the migration behavior of coarse aggregates in the compaction process of asphalt mixtures, the "Intelligent Aggregate Attitude Acquisition System (IAS)" is developed based on 3D printing technology and wireless intelligent sensing technology, and the "Intelligent Attitude Aggregate (IAA)" is prepared as the acquisition terminal. The Superpave Gyratory Compaction (SGC) test and the Internet of Things (IOT) wireless sensor technology are combined to collect and analyze the attitude data of an SMA-20 asphalt mixture built in IAA at different compaction stages, and the migration behavior of coarse aggregate in the compaction process is quantitatively characterized. The result shows that the IAA is suitable as a "tracking aggregate" to study the aggregate transfer behavior in asphalt mixtures. The IAA in the upper layer tends to move vertically downward, while the particles in the lower layer tend to move horizontally and spatial rotation in the process of rotating compaction. With the increase in asphalt content, the lubrication effect between aggregate particles is obvious, and the friction resistance of aggregate particles decreases when it is embedded downward. Affected by shear force in the process of rotary compaction, the aggregate particles are easier to overcome friction and cause large horizontal migration and spatial rotation. With the increase in compaction temperature, the viscosity of asphalt binder decreases, and the contact friction between aggregate particles decreases. The asphalt content has a significant effect on the displacement in the horizontal plane D_{xoy} of the aggregate. The asphalt content and compaction temperature have significant effects on the spatial rotation angle Φ of aggregate, but the asphalt content has a greater impact on it.

Keywords: highway engineering; asphalt mixture; aggregate; migratory behavior; intelligent acquisition system; attitude data

check for updates

Citation: Zhang, C.; Zhang, Z. Study on Migratory Behavior of Aggregate in Asphalt Mixture Based on the Intelligent Acquisition System of Aggregate Attitude Data. *Sustainability* **2021**, *13*, 3053. https://doi.org/10.3390/su13063053

Academic Editor: Davide Lo Presti

Received: 19 February 2021
Accepted: 8 March 2021
Published: 11 March 2021

1. Introduction

Complicated particle migration and friction behaviors occur during the compaction process of asphalt mixtures, which is also the essential manifestation of the compaction characteristics of asphalt mixtures [1]. Relevant studies have shown that the compaction quality of asphalt pavement is closely related to the contact and interlock behavior between aggregates [2]. In the laboratory test, the Superpave Gyratory Compactor (SGC) can be used to characterize the correlation between the compaction characteristics of the asphalt mixture and the particle contact behavior, but it is difficult to accurately reveal the mechanism of aggregate skeleton formation in asphalt mixtures [3].

Zhang used SK70# and SK90# matrix asphalt and limestone to prepare asphalt mixtures via Superpave Gyratory Compaction (SGC) and X-ray CT Scanning to determine the appropriate compaction parameters of different asphalt mixtures and to study their microstructural characteristics [4]. Kim examined the effect of compaction temperature on the volumetric properties and the compaction energy indices to determine a proper compaction temperature that affects the workability and compatibility of the polymer-modified asphalt (PMA) [5]. Gong analyzed the movement characteristic of differently shaped compositions in the Superpave gyratory compactor (SGC) test through tracking coarse aggregates and a numerical simulation of the Discrete Element Method (DEM) [6]. Pouranian developed a framework to define the aggregate structure of asphalt mixtures when fine and coarse aggregate stockpiles are blended [7]. Olsson developed a new DEM modelling approach for studying the asphalt compaction process, incorporating contact and damage laws based on granular mechanics [8]. Li conducted step-by-step gyratory compactions on the asphalt mixtures with different gradations under different test conditions to anatomize the migration properties of aggregates during the compaction process of asphalt mixtures [9]. Huang used the principal axis orientation and interlayer distance as evaluation indicators obtained by digital image processing (DIP) and Image-Pro Plus (IPP) software to evaluate the migration characteristics of aggregate particles in asphalt mixtures [10]. Qian traced the air void (AV) content and distribution of aggregates and asphalt mortar in the process of asphalt mixture compaction to capture the mesostructural change characteristics of asphalt mixtures during compaction [11]. Cai characterizes the skeleton characteristics of asphalt mixtures under various cycles of compaction repetitions by introducing coarse aggregate contact points, aggregate inclination and some other indexes based on a digital image processing technique [12]. Almusawi investigated existing alternative methods which can be suitable for estimating the mixing and compaction temperatures of both warm mix asphalt (WMA) and polymer-modified bitumen (PMB) mixtures [13].

It can be seen that the research in this field mainly focuses on the analysis of the compaction characteristics of asphalt mixtures through the macroscopic characteristics of the compaction process or use of nondestructive scanning technology to analyze the microstructure of the compacted specimen. There are few studies on quantitatively characterizations of the migration behavior of coarse aggregates during the compaction process of asphalt mixtures based on wireless sensing technology of the Internet of Things (IOT). Based on this, a device was developed in this article that uses 3D printing technology and wireless intelligent perception technology called "Intelligent acquisition system of aggregate attitude data (IAS)" and an "Intelligent Attitude Aggregate (IAA)" which are prepared based on the real aggregate form. Combining the Superpave gyratory compactor (SGC) and the wireless sensing technology, the attitude data at different compaction stages of the SMA-20 grading asphalt mixture built in IAA are collected and analyzed, respectively, which could quantitatively characterize the migration behavior of coarse aggregates during the compaction process.

2. Method

To facilitate tracking of the compaction state of the mixture, the SGC was used for the preparation of SMA-20 specimens, and based on the "IAS", the internal aggregate attitude data of asphalt mixtures in different compaction stages were collected and analyzed.

2.1. System Development of IAS

Based on remote wireless transmission technology, 3D printing technology, computer programming technology, high-temperature-resistant materials (mainly composed of epoxy putty), and MPU6050 attitude sensors, the IAS system was developed. The system includes three parts: intelligent attitude aggregate (IAA), analysis software and hardware equipment, which are introduced in the following.

2.1.1. Intelligent Attitude Aggregate (IAA)

The MPU6050 attitude sensor, rechargeable microbatteries and wireless transmission modules were used to prepare IAA with a particle size of 20 mm. The encapsulation process of IAA based on 3D printing technology (control shape), high-strength and high-temperature-resistant materials (to ensure material strength and signal stability) can ensure the IAA wireless communication at a long distance (within 100 m) in a closed environment at 200 °C. The customized large-capacity microbatteries module can ensure that the IAA works continuously for 72 h and has remote power-on and power-off functions. If the IAA data are collected regularly, the battery life will be longer. The IAA can output data of its own three-axis acceleration and three-axis spatial attitude angle. The preparation process is shown in Figure 1.

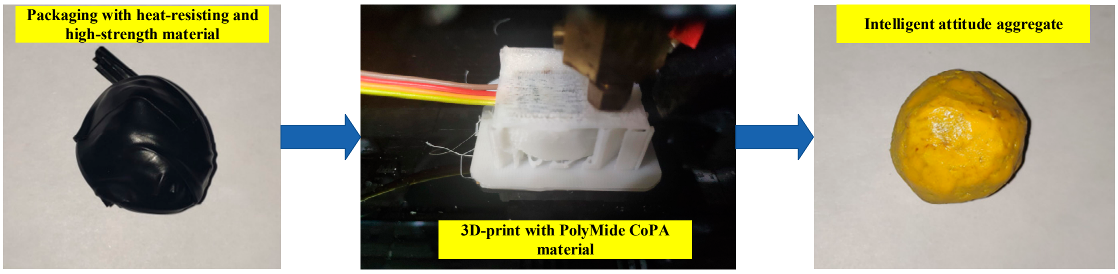

Figure 1. Preparation process of Intelligent Attitude Aggregate (IAA).

Comparison of technical properties between IAA and traditional limestone aggregates is shown in Table 1.

Table 1. Comparison of technical properties between IAA and traditional limestone aggregates.

Index	Units	Limestone Aggregate	IAA	Technical Standard	Test Method
Crushing value	%	22.5	18.6	≤28	T0316
Wear value	%	21.6	17.6	≤30	T0317
Compressive strength	MPa	61.3	66.8	≥50	T0616

From Table 1, the indicators of IAA and limestone aggregate are close and can replace traditional aggregates as they can withstand external load and internal load transfers. The mixing and molding temperature of asphalt mixtures generally does not exceed 200 °C. In this paper, the IAA is placed in a temperature box to perform high-temperature resistance tests under different temperature conditions (25 °C, 50 °C, 75 °C, 100 °C, 125 °C, 150 °C, 175 °C, 200 °C), and then test the compressive strength value of IAA at each temperature level. The results are shown in Figures 2 and 3.

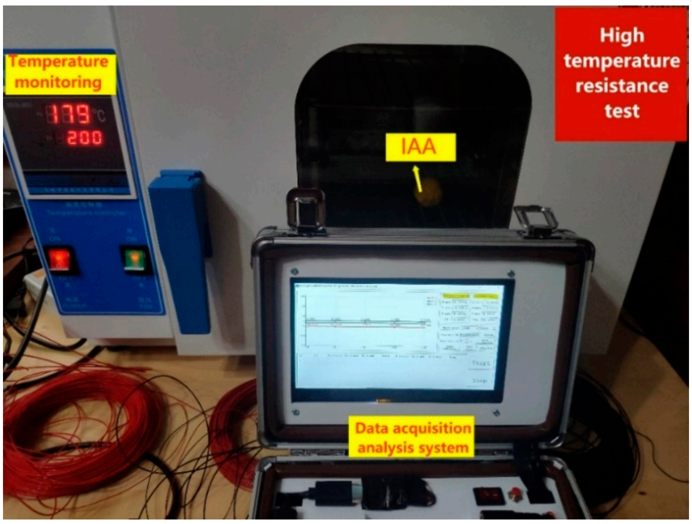

Figure 2. High-temperature resistance test of IAA.

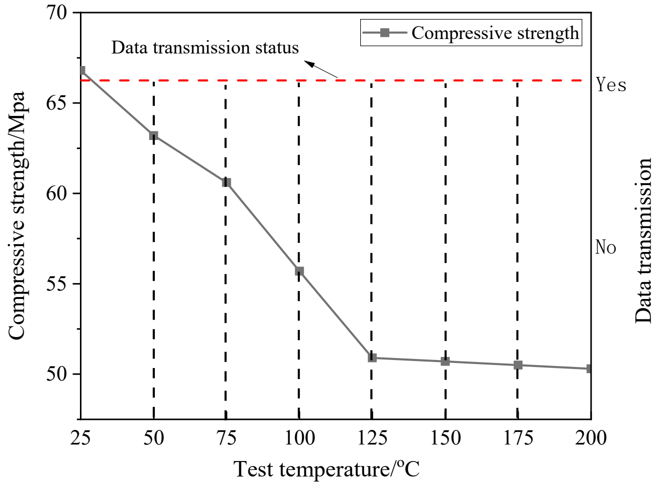

Figure 3. High-temperature resistance test result of IAA.

As can be seen in Figures 2 and 3, the IAA can conduct reliable data transmission within 200 °C, but its compressive strength decreases with the increase in temperature and reaches a stable state. This is because the IAAs are 3D printing layers, epoxy putty layers, and chipsets wrapped by thermal insulation material from the outside to the inside [14]. When the temperature reaches 125 °C, the 3D printing layer is destroyed under the load, but the epoxy putty layer has excellent thermal insulation and strength properties, which can ensure that the IAA has stable compressive strength and data transmission capabilities.

2.1.2. Software

The software can realize the timing collection of data and real-time algorithm analysis, and the collected data can be saved as an excel file in real time, as shown in Figure 4.

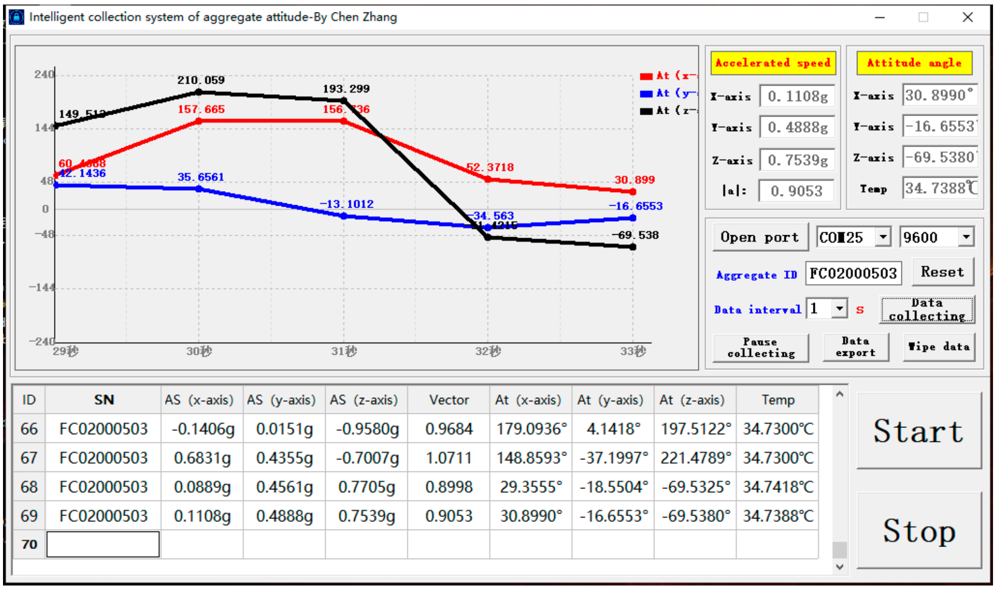

Figure 4. Software of Intelligent Aggregate Attitude Acquisition System (IAS).

2.1.3. Hardware

The hardware mainly includes a module, remote power control module for IAA, data processing system and display screen, as shown in Figure 5.

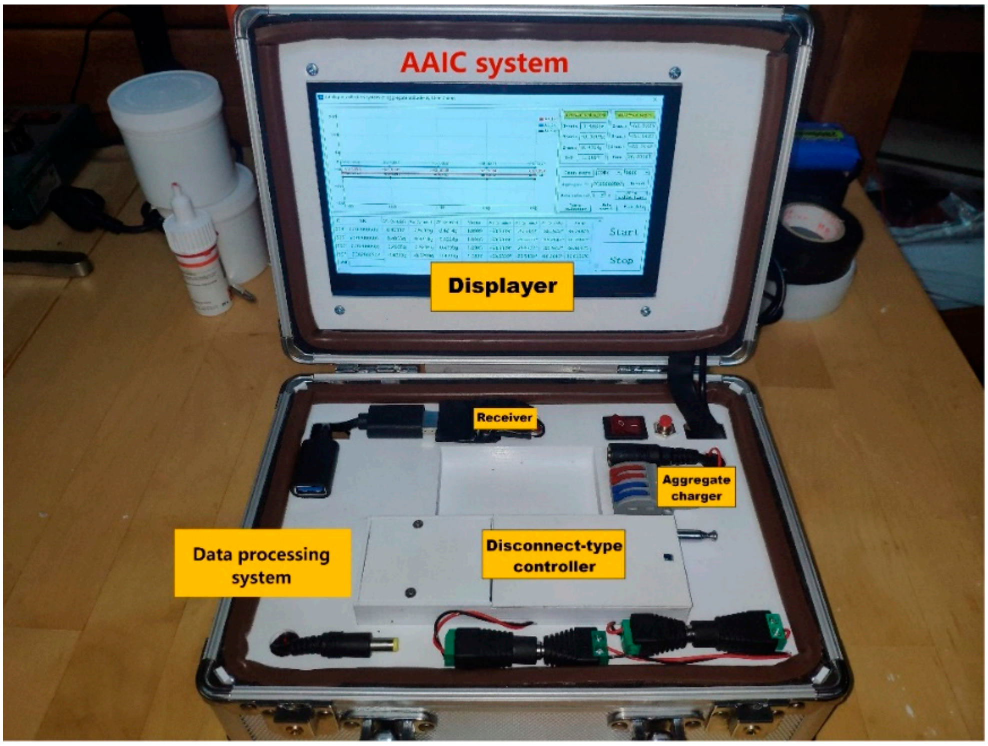

Figure 5. Hardware of IAS.

2.2. Algorithm Analysis and Correction of Spatial Displacement for IAA

This paper obtains the acceleration and attitude angles of IAA and uses the laser displacement sensor to obtain its displacement in the X-scale, Y-scale and Z-scale at the same time. The data collection interval is 1 s. Multiple linear regression analysis was performed with 10,000 sets of data and the relationship between the space displacement and attitude parameter of IAA was obtained, as shown in Equation (1).

$$\begin{cases} D_x = 11.216 + 0.748x_1 + 2.092x_2 - 1.459x_3 + 0.031x_4 - 0.02x_5 - 0.009x_6 \\ D_y = 11.813 + 0.05x_1 + 1.615x_2 - 0.971x_3 + 0.042x_4 - 0.012x_5 - 0.009x_6 \\ D_z = 8.651 - 0.555x_1 + 0.114x_2 - 0.925x_3 + 0.023x_4 - 0.027x_5 - 0.01x_6 \end{cases} \quad (1)$$

In Formula (1), D_x, D_y and D_z are the displacements in three directions, respectively; x_1 is x-axis accelerated speed at the starting point of displacement; x_2 is y-axis accelerated speed at starting point of displacement; x_3 is z-axis accelerated speed at starting point of displacement; x_4 is x-axis attitude angle, x_5 is y-axis attitude angle, x_6 is z-axis attitude angle, where x_4~x_6 are the difference values of the start-point and end-point of displacement (absolute value). The X-ray CT nondestructive scanning system can obtain three-dimensional images of asphalt mixture specimens built in IAA, and the spatial displacement of IAA can be measured combined with Image-Pro Plus (IPP) analysis software, as shown in Figure 6. This paper uses the X-ray CT nondestructive scanning system and IPP analysis software to measure the spatial displacement of the IAA in the compacted specimens in experiment process to verify and correct the regression—Equation (1).

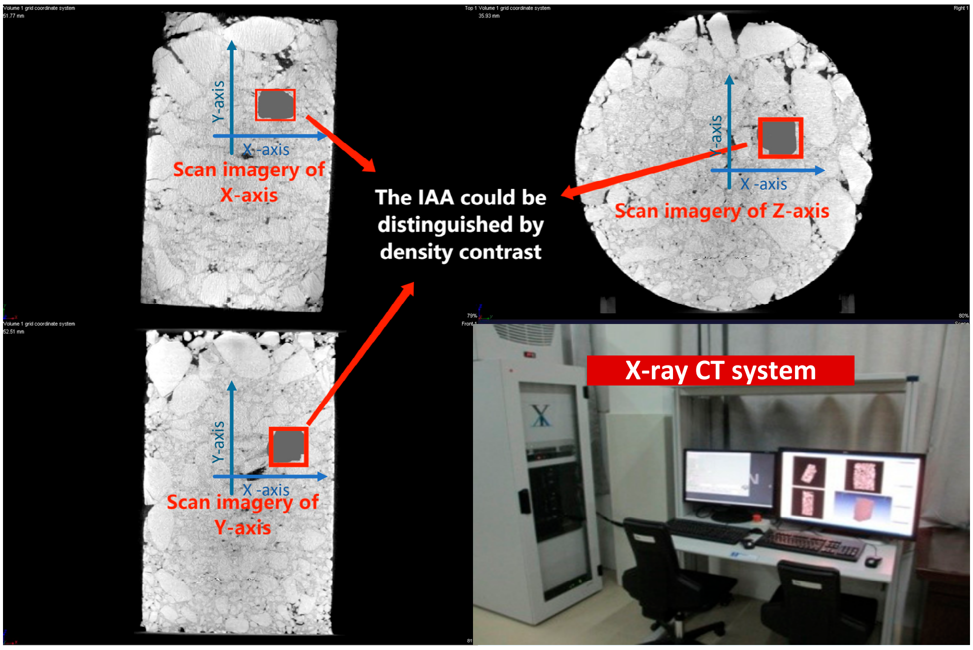

Figure 6. Measured of IAA spatial displacement with X-ray CT.

The test used three groups of parallel specimens, and the final results were averaged. Firstly, IAA was used to collect and analyze the data of specimens in different rotary compaction stages. At the same time, CT scanning and image analysis were carried out on the corresponding specimens to verify the displacement calculation results of IAA, and then the attitude analysis of IAA and the quantitative characterization of mixture compaction process were completed [15]. When the specimen was not compacted, two IAAs were arranged as the N_0 state. IAA data were collected after 8 compactions, and the specimens were taken out for CT scanning, denoted as the N_8 state. After 8-time srotary compaction, the IAA data were collected, and the specimen was taken out for CT scanning, which was denoted as the N_8 state. Then, the specimen was reheated and loaded with the mold again to continue compaction, so as to deduce other stages.

This paper uses Equations (2) and (3) to calculate the attitude data of IAA.

$$D_{xoy} = \sqrt{D_x{}^2 + D_y{}^2 + D_z{}^2} \tag{2}$$

$$\Phi = \sqrt{\Phi_{\Delta x}{}^2 + \Phi_{\Delta y}{}^2 + \Phi_{\Delta z}{}^2} \tag{3}$$

In Equations (2) and (3), D_x (mm) is the displacements in x-axis directions, a negative values represents the opposite direction; D_y (mm) is the displacements in y-axis directions; D_z (mm) is the displacements in z-axis directions; D_{xoy} (mm) is the displacements in the horizontal plane; $\Phi_{\Delta x}$ is the x-axis attitude angle after compaction; $\Phi_{\Delta y}$ is the y-axis attitude angle after compaction; $\Phi_{\Delta z}$ is the z-axis attitude angle after compaction; Φ is the space attitude angle after compaction.

The posture of IAA was calibrated before compaction so as to compare the IAA posture of the final rotary compaction. In order to describe the vertical displacement law of IAA more reliably, the vertical relative displacement S was used for characterization, as shown in Equation (4).

$$S = D_z/\Delta h \tag{4}$$

where S is the relative value of the vertical downward displacement, Δh is the height change value (mm) of the specimen after compaction, and D_z is the vertical downward displacement (mm) of IAA during the compaction process.

2.3. Research Scheme

An SGC was used to mold specimens. The IAA posture data at different layers in the SMA-20 asphalt mixture were collected and analyzed based on the IAS. The X-ray CT nondestructive scanning system was used to verify Equation (1). The compacting process of the asphalt mixture was quantitatively characterized and its influencing factors were analyzed. The overall technical scheme of this paper is shown in Figure 7.

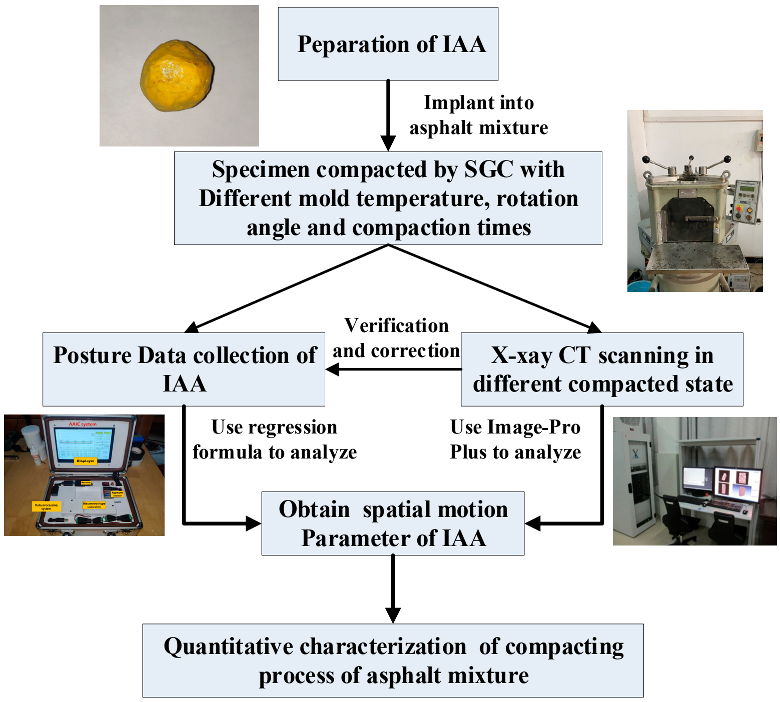

Figure 7. Testing plan.

3. Material

3.1. Test Material Preparation

The SMA-20 gradation, 90# matrix asphalt, limestone aggregate, and 6.0% oil-stone ratio were used, and some cylindrical specimens of the asphalt mixture with 100 mm diameters and 150 mm heights were molded by SGC. The molding temperature was 175 °C and the rotation angle was 1°. Two IAAs were implanted in the asphalt mixture, and the placement state is shown in Figure 8.

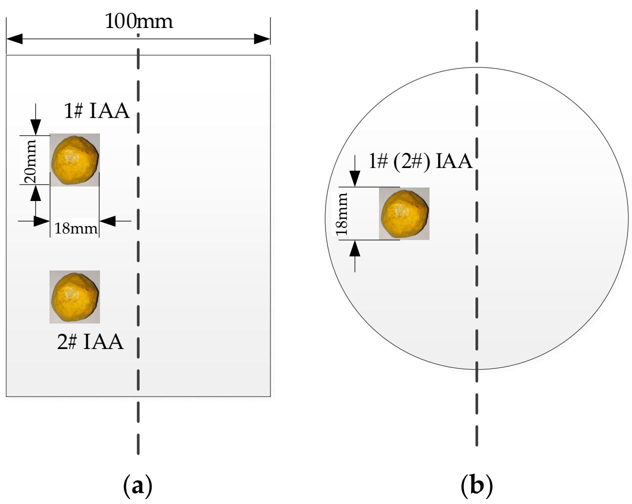

Figure 8. Schematic diagram of IAA distribution: (**a**) Sectional view and (**b**) Vertical view.

According to the above-mentioned specimen preparation parameters, two groups of asphalt mixture specimens were prepared. Each group of specimens had three parallel specimens, of which group A are ordinary specimens, and group B are specimens built in IAA. Based on the "Standard Test Methods of Bitumen and Bituminous Mixtures for Highway Engineering (JTGE20-2011)", the UTM30 testing machine was used to conduct uniaxial compression tests on two sets of specimens to determine the compression rebound modulus and compressive strength of them [16]. The test temperature was 25 °C, the loading rate was 2 mm/min, and the test results were averaged. The results are shown in Table 2.

Table 2. Comparison of the uniaxial compression test result.

Index	Test Results		Difference
	Group A	Group B	
Compression rebound modulus	1125 Mpa	1097 Mpa	2.5%
Compressive strength	4.13 Mpa	3.96 Mpa	4.1%

From Table 2, the performance difference of the asphalt mixture built in IAA and ordinary asphalt mixture is within 5%, which meets the specification requirements [17]. The IAA is made based on the real aggregate shape, so implanting the IAA into the asphalt mixture could not significantly affect its original gradation and mechanical properties.

3.2. Test Procedure

The three SMA-20 asphalt mixture specimens were molded, where the compaction times was N_{ini} = 8, the design compaction time was N_{des} = 100, and the maximum compaction times was N_{max} = 160. The density ratio under the design compaction times is γ = 96%, and the rotary compaction curve is shown in Figure 9.

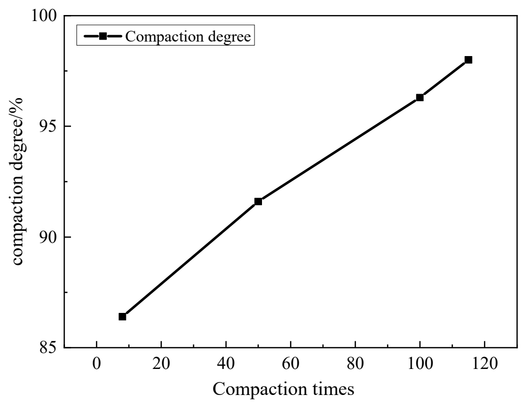

Figure 9. Rotary compaction curve of SMA-20 asphalt mixture.

The compaction degree in Figure 9 is the average value of three parallel specimens. In Figure 8, it can be seen that the compaction degree reached 86.4% after 8 compactions, 91.6% after 50 compactions, 96.3% after 100 compactions, and reached 98% after 115 compactions. Based on this, in order to better reflect the different compaction states of asphalt mixtures, this paper uses 8 compactions as the first stage, 50 compactions as the second stage, and 115 compactions as the third stage [18]. The compaction scheme is shown in Table 3.

Table 3. Compaction scheme.

Compaction Stage	Compaction Times	Compaction State
1	N = 8	Accumulative compaction (8 times)
2	N = 50	Continue the compaction (42 times) and Accumulative compaction (50 times)
3	N = 115	Continue to the compaction (65 times) and Accumulative compaction (115 times)

4. Test Results and Discussion

4.1. Data Verification

Referring back to Section 2.2, the IAA attitude data obtained by the two methods were compared, and the results are shown in Table 4.

Table 4. Space attitude changes of IAA after compaction.

Index	Data Result by IAA						Data Result by CT Scanning					
	1# IAA			2# IAA			1# IAA			2# IAA		
	N_8	N_{50}	N_{115}	N_8	N_{50}	N_{115}	N_8	N_{50}	N_{115}	N_8	N_{50}	N_{115}
D_x/mm	5.2	2.1	1.2	7.6	4.1	1.1	6.8	1.9	0.7	8.9	4.8	1.2
D_y/mm	−4.6	−3.7	−0.9	7.2	−4.8	−0.9	−5.2	−4.2	−1.1	8.2	−4.3	−0.7
D_z/mm	−7.8	−6.1	−1.5	−7.9	3.6	−0.9	−7.3	−5.7	−1.2	−8.6	4.5	−0.6
D_{xoy}/mm	10.4	7.4	2.1	13.1	7.3	1.7	11.3	7.3	3.1	14.8	7.9	2.3
$\Phi_{\Delta x}/°$	61.6	10.3	3.4	63.5	12.5	4.3	-	-	-	-	-	-
$\Phi_{\Delta y}/°$	−52.2	−8.6	−2.2	−56.6	−9.8	−5.3	-	-	-	-	-	-
$\Phi_{\Delta z}/°$	−35.5	6.4	1.8	−26.5	7.2	2.7	-	-	-	-	-	-
$\Phi/°$	88.2	14.9	4.4	89.1	17.4	7.3						

SPSS two-factor variance analysis was used to determine whether the displacement data obtained by the two methods have differences, as shown in Table 5.

Table 5. Comparison of displacement results.

Index	1# IAA			2# IAA		
	F	*p*-Value	F Crit	F	*p*-Value	F Crit
D_x/mm	5.33	0.087	6.54	5.21	0.092	7.35
D_y/mm	6.72	0.143	7.95	8.77	0.123	11.23
D_z/mm	9.51	0.076	11.5	6.73	0.174	8.82
D_{xoy}/mm	7.85	0.092	10.6	7.74	0.147	9.33

According to the assumptions of SPSS two-factor variance analysis, if F < Fcrit, and $p > 0.05$, it indicates that there is no difference between the two groups of data. From Table 5, the *p*-values of each comparison index are greater than 0.05. It can be seen that the results obtained by the IAA displacement calculation formula are not different from those obtained by X-ray CT image processing [19]. The displacement calculation formula based on the regression of IAA attitude data has high reliability.

4.2. Test Results Analysis

4.2.1. Analysis of Migration Behavior of Aggregate during Compaction

According to the attitude data in Table 4, the displacement index and angle index of IAA were obtained. To facilitate analysis, all values are positive, as shown in Figures 10 and 11.

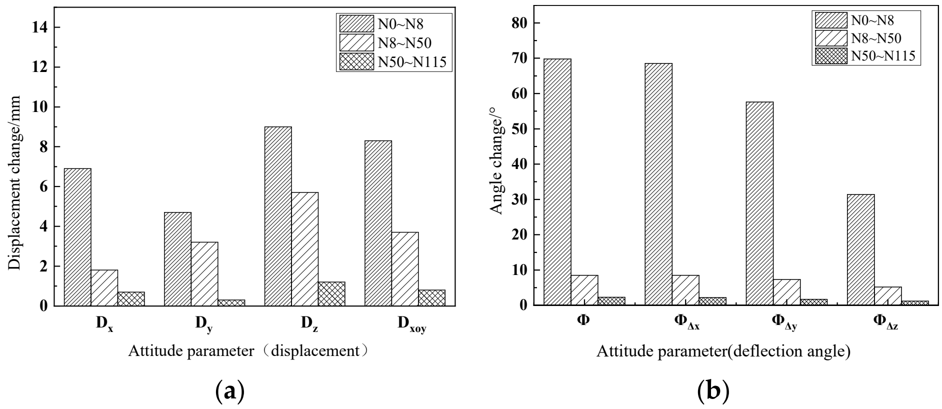

Figure 10. Displacement and angle changes in different compaction stages (1# IAA): (**a**) Displacement changes of 1# IAA and (**b**) Angle changes of 1# IAA.

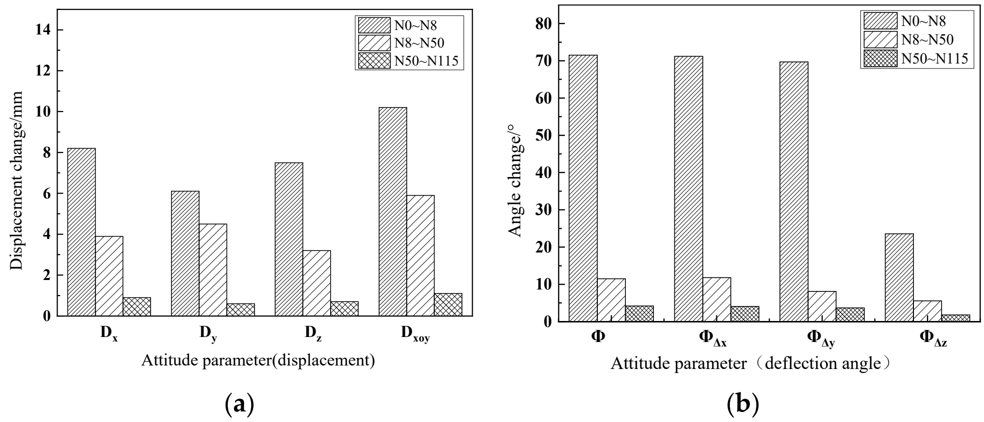

Figure 11. Displacement and angle changes in different compaction stages (2# IAA): (**a**) Displacement changes of 2# IAA and (**b**) Angle changes of 2# IAA.

From Figures 10a and 11a, the displacements in z-axis directions D_z of 1# IAA are larger than 2# IAA at each compaction stage. This shows that the 2# IAAs in lower layers are more difficult to move downward in the asphalt mixture as it becomes gradually denser. At the same time, the displacements in the z-axis directions D_z of 1# IAA in the upper layer at each compaction stage is greater than that in the horizontal plane D_{xoy}, while the displacements in horizontal plane D_{xoy} of 2# IAA in the lower layer at each compaction stage are greater than that in in z-axis directions D_z.

It was concluded that during the whole compaction process, for the aggregate with 20 mm particle size in the asphalt mixture, the aggregate in the middle and upper layer mainly underwent downward displacement, while the aggregate in the middle and lower layer mainly underwent horizontal displacement [20].

From Figures 10b and 11b, the spatial rotation angle Φ of 1# IAA is smaller than that of 2# IAA in each stage of compaction. For 1# IAA and 2# IAA, the x-axis attitude angle after compaction $\Phi_{\Delta x}$ is the largest, and the z-axis attitude angle after compaction $\Phi_{\Delta z}$ is the smallest. It can be seen that in the process of rotary compaction, the aggregate of 20 mm particle size exhibits significant spatial rotation, but this rotation tends to be mainly translational, while the vertical rotation is smaller.

In summary, in the process of rotary compaction, the coarse aggregate particles will exhibit rolling and migration behaviors under external force. The coarse aggregate in the middle and upper layers tends to migrate vertically downward, while the particles in the middle and lower layers tend to migrate horizontally and move spatially.

4.2.2. Analysis of Influencing Factors of Aggregate Migration

Referring to Section 2.1, the same specifications of asphalt mixture specimens containing IAA were prepared to ensure that the test operation is consistent and the data are comparable [21].

(1) Effect of asphalt content on migration of coarse aggregate.

The different asphalt contents (5.2%, 5.8%, 6.4%) were used to mold SMA-20 asphalt mixture specimens and calculate the migration indicators of IAA in SMA-20 asphalt mixture with different asphalt contents. The results are shown in Table 6.

Table 6. Migration indicators of IAA in SMA-20 asphalt mixture.

Asphalt Content	Indicator	1# IAA	2# IAA
5.2%	S	1.03	0.36
	D_{xoy}/mm	8.5	11.6
	Φ/°	66.7	73.4
5.8%	S	1.62	0.71
	D_{xoy}/mm	14.7	19.7
	Φ/°	89.7	92.5
6.4%	S	2.06	0.96
	D_{xoy}/mm	22.5	27.4
	Φ/°	102.5	113.6

SPSS one-way analysis of variance was used to study the influence of asphalt content on each migration indicator of coarse aggregate, and the significance level was 0.05. The results are shown in Table 7.

Table 7. Influence weight analysis of asphalt content on migration indicators of coarse aggregate.

Independent Variable	Dependent Variable	*F*-Value	*p*-Value
Asphalt content	S	0.808	0.524
	D_{xoy}/mm	11.368	0.04
	Φ/°	24.718	0.014

It can be seen from Tables 6 and 7 that with the increase in asphalt content, the vertical relative displacement S, horizontal displacement D_{xoy} and spatial rotation angle Φ of the two IAAs increased. The extent to which vertical relative displacement S of 1# IAA increased in the upper layer is larger than that of 2# IAA particles in the lower layer. This shows that with the increase in asphalt content, the lubrication effect between aggregate particles is obvious, and the friction resistance of aggregate particles decreases when it is embedded downward, which makes it easier to move downward to a deeper position [22].

The displacement of 2# IAA in the middle and lower layers is relatively small due to the decrease in compressive stress with depth. The vertical displacement of 2# IAA in the middle and lower layers is relatively small due to the decrease in compressive stress with depth. With the increase in asphalt content, due to the influence of shear force during compaction, aggregate particles are easier to overcome friction and cause large horizontal migration and spatial rotation [23].

The variance analysis shows that the asphalt content has a significant effect on the spatial rotation angle Φ and the displacement in horizontal plane D_{xoy} of aggregate, especially on the spatial rotation angle Φ of the aggregate ($p = 0.014 < 0.05$).

(2) Effect of compaction temperature on particle migration.

SMA-20 asphalt mixture was compacted under three different compaction temperatures of 140 °C, 160 °C and 175 °C, and the attitude data of IAA in each specimen were calculated. The results are shown in Table 8.

Table 8. The attitude data of IAA under different compaction temperatures.

Compaction Temperatures	Index	1# IAA	2# IAA
140 °C	S	0.72	0.29
	D_{xoy}/mm	9.2	14.8
	Φ/°	71.6	78.4
160 °C	S	1.27	0.37
	D_{xoy}/mm	13.3	18.7
	Φ/°	88.3	98.5
175 °C	S	1.86	0.49
	D_{xoy}/mm	17.5	22.4
	Φ/°	103.6	112.3

The SPSS one-way variance analysis was used to study the influence weight of compaction temperature on each migration index of IAA. The significance level was 0.05 and the results are shown in Table 9.

Table 9. Weight analysis of influence of compaction temperature on migration indexes of coarse aggregate.

Independent Variable	Dependent Variable	*F*-Value	*p*-Value
Compaction temperature	S	0.2	0.829
	D_{xoy}/mm	2.243	0.254
	Φ/°	14.479	0.029

It can be seen from Tables 8 and 9 that with the increase in compaction temperature, the viscosity of asphalt binder decreases, and the contact friction between aggregate particles decreases. The vertical relative displacement S, the displacement in horizontal plane D_{xoy} and the spatial rotation angle Φ of two IAAs are all increased. The increase in vertical relative displacement S of 1# IAA in the upper layer is greater than that of 2# IAA in the lower layer. For the displacement in horizontal plane D_{xoy} and the spatial rotation angle Φ, the index value of 2# IAA in the lower layer is greater than that of 1# IAA in the upper layer. This is because the compressive stress of 2# IAA in the lower layer is relatively small, and the lower part of the specimen will reach the target density first rather than the upper part, which causes the 2# IAA in the lower layer to be more prone to horizontal displacement and spatial rotation. The variance analysis shows that the compaction temperature has a significant effect on the spatial rotation angle Φ ($p = 0.029 < 0.05$).

5. Conclusions

Based on 3D printing technology and wireless intelligent sensing technology, the intelligent collection system of aggregate attitude (IAS) was developed, and the intelligent attitude aggregate (IAA) with particle size of 20 mm based on the real aggregate morphology was prepared. The IAA has a similar shape and mechanical properties to traditional aggregates, and can be used for wireless data acquisition of triaxial acceleration and spatial attitude angle in a closed environment at 200 °C. The implantation of IAA in asphalt mixture does not have a significant impact on its original gradation and mechanical properties. IAA is a suitable "tracking aggregate" to study aggregate transfer behavior in asphalt mixtures.

A method is proposed to calculate the spatial displacement of aggregates by using the spatial attitude parameters of IAA. The coarse aggregate particles will roll and pile up under the action of external force in the process of rotating compaction. The IAA in the upper layer tends to move vertically downward, while the particles in the lower layer tend to move horizontally and undergo spatial rotation.

With the increase in asphalt content, the lubrication effect between aggregate particles is obvious, and the friction resistance of aggregate particles decreases when they are embedded downward. The process of rotary compaction is affected by shear force, which makes it easier for the aggregate particles to overcome friction and cause large horizontal migration and spatial rotation. With the increase in compaction temperature, the viscosity of asphalt binder decreases, and the contact friction between aggregate particles decreases. The asphalt content has a significant effect on the displacement in the horizontal plane D_{xoy} of aggregate. The asphalt content and compaction temperature have significant effects on the spatial rotation angle Φ of aggregate, but the asphalt content has a greater impact on it.

Using IAS to quantitatively characterize the migration state of aggregate in the compaction process of asphalt mixtures has a high efficiency and high accuracy. The research results of this paper also provide a new method for characterizing the compaction quality of asphalt pavement.

Author Contributions: Investigation, Z.Z.; Methodology, C.Z.; Software, C.Z.; Validation, Z.Z. All authors have read and agreed to the published version of the manuscript.

Funding: This research was funded by the China Postdoctoral Science Foundation (2020M683402), Open Fund of Key Laboratory for Special Area Highway Engineering of Ministry of Education (Chang'an University) (300102210504), and the Science and Technology Planning Project of Xi'an (2020KJRC0046).

Institutional Review Board Statement: Not applicable.

Informed Consent Statement: Not applicable.

Data Availability Statement: The data presented in this study are available on request from the corresponding author. The data are not publicly available due to privacy.

Conflicts of Interest: The authors declare no conflict of interest.

References

1. Pouranian, M.R.; Shishehbor, M.; Haddock, J.E. Impact of the coarse aggregate shape parameters on compaction characteristics of asphalt mixtures. *Powder Technol.* **2020**, *363*, 369–386. [CrossRef]
2. Manzi, S.; Mazzotti, C.; Bignozzi, M.C. Self-compacting concrete with recycled concrete aggregate: Study of the long-term properties. *Constr. Build. Mater.* **2017**, *157*, 582–590. [CrossRef]
3. Li, J.; Zhang, J.; Qian, G.; Zheng, J.; Zhang, Y. Three-dimensional simulation of aggregate and asphalt mixture using parameterized shape and size gradation. *J. Mater. Civil. Eng.* **2019**, *31*, 04019004. [CrossRef]
4. Zhang, C.; Wang, H.; You, Z.; Yang, X. Compaction characteristics of asphalt mixture with different gradation type through Superpave Gyratory Compaction and X-ray CT Scanning. *Constr. Build. Mater.* **2016**, *129*, 243–255. [CrossRef]
5. Kim, K.; Kang, M. Effects of compaction temperature on the volumetric properties and compaction energy efforts of polymer-modified asphalt mixtures. *J. Wuhan Univ. Technol. Mater. Sci. Ed.* **2018**, *33*, 146–154. [CrossRef]
6. Gong, F.; Zhou, X.; You, Z.; Liu, Y.; Chen, S. Using discrete element models to track movement of coarse aggregates during compaction of asphalt mixture. *Constr. Build. Mater.* **2018**, *189*, 338–351. [CrossRef]
7. Pouranian, M.R.; Haddock, J.E. A new framework for understanding aggregate structure in asphalt mixtures. *Int. J. Pavement Eng.* **2019**, 1–17. [CrossRef]
8. Olsson, E.; Jelagin, D.; Partl, M.N. New discrete element framework for modelling asphalt compaction. *Road Mater. Pavement* **2019**, *20*, 604–616. [CrossRef]
9. Li, P.; Su, J.; Gao, P.; Wu, X.; Li, J. Analysis of aggregate particle migration properties during compaction process of asphalt mixture. *Constr. Build. Mater.* **2019**, *197*, 42–49. [CrossRef]
10. Huang, J.; Pei, J.; Li, Y.; Yang, H. Investigation on aggregate particles migration characteristics of porous asphalt concrete (PAC) during vibration compaction process. *Constr. Build. Mater.* **2020**, *243*, 118153. [CrossRef]
11. Qian, G.; Hu, K.; Li, J.; Bai, X.; Li, N. Compaction process tracking for asphalt mixture using discrete element method. *Constr. Build. Mater.* **2020**, *235*, 117478. [CrossRef]
12. Cai, X.; Wu, K.; Huang, W. Study on the optimal compaction effort of asphalt mixture based on the distribution of contact points of coarse aggregates. *Road Mater. Pavement* **2020**, 1–22. [CrossRef]
13. Almusawi, A.; Sengoz, B.; Topal, A. Evaluation of mechanical properties of different asphalt concrete types in relation with mixing and compaction temperatures. *Constr. Build. Mater.* **2021**, *268*, 121140. [CrossRef]
14. Wang, J.; Liu, Y.; Fan, Z.; Wang, W.; Wang, B.; Guo, Z. Ink-based 3D printing technologies for graphene-based materials: A review. *Adv. Compos. Hybrid Mater.* **2019**, *2*, 1–33. [CrossRef]
15. Liu, W.; Gao, Y.; Huang, X.; Li, L. Investigation of motion of coarse aggregates in asphalt mixture based on virtual simulation of compaction test. *Int. J. Pavement Eng.* **2020**, *21*, 144–156. [CrossRef]

16. Antunes, V.; Freire, A.C.; Neves, J. A review on the effect of RAP recycling on bituminous mixtures properties and the viability of multi-recycling. *Constr. Build. Mater.* **2019**, *211*, 453–469. [CrossRef]
17. Ministry of Transport of the People's Republic of China. *Test Methods of Aggregate for Highway Engineering: JTG E42-2005*; China Communications Press: Beijing, China, 2005.
18. Liu, P.; Xu, H.; Wang, D.; Wang, C.; Schulze, C.; Oeser, M. Comparison of mechanical responses of asphalt mixtures manufactured by different compaction methods. *Constr. Build. Mater.* **2018**, *162*, 765–780. [CrossRef]
19. Xing, C.; Xu, H.; Tan, Y.; Liu, X.; Zhou, C.; Scarpas, T. Gradation measurement of asphalt mixture by X-ray CT images and digital image processing methods. *Measurement* **2019**, *132*, 377–386. [CrossRef]
20. Ma, T.; Zhang, D.; Zhang, Y.; Wang, S.; Huang, X. Simulation of wheel tracking test for asphalt mixture using discrete element modelling. *Road Mater. Pavement* **2018**, *19*, 367–384. [CrossRef]
21. Ciampa, D.; Cioffi, R.; Colangelo, F.; Diomedi, M.; Farina, I.; Olita, S. Use of unbound materials for sustainable road infrastructures. *Appl. Sci.* **2020**, *10*, 3465. [CrossRef]
22. Li, P.; Su, J.; Ma, S.; Dong, H. Effect of aggregate contact condition on skeleton stability in asphalt mixture. *Int. J. Pavement Eng.* **2020**, *21*, 196–202. [CrossRef]
23. Su, J.; Li, P.; Wei, X.; Zhu, L.; Gao, J. Interface Transformation Behavior of Bonding/Lubrication of Aggregate-Asphalt System. *J. Mater. Civil. Eng.* **2020**, *32*, 04020380. [CrossRef]